Hydrological consequences of Eucalyptus afforestation in the Argentine Pampas

Hydrological consequences of Eucalyptus afforestation in the Argentine Pampas

Vic Engel,[1] Esteban G. Jobbágy,[2,3] Marc Stieglitz,[4] Mathew Williams,[5] and Robert B. Jackson[3,6]

Received 25 October 2004; revised 6 May 2005; accepted 15 June 2005; published 14 October 2005.

[1] The impacts of a 40 ha stand of *Eucalyptus camaldulensis* in the Pampas grasslands of Argentina were explored for 2 years using a novel combination of sap flow, groundwater data, soil moisture measurements, and modeling. Sap flow measurements showed transpiration rates of 2–3.7 mm d^{-1}, lowering groundwater levels by more than 0.5 m with respect to the surrounding grassland. This hydraulic gradient induced flow from the grassland areas into the plantation and resulted in a rising of the plantation water table at night. Groundwater use estimated from diurnal water table fluctuations correlated well with sap flow ($p < 0.001$, $r^2 = 0.78$). Differences between daily sap flow and the estimates of groundwater use were proportional to changes in surface soil moisture content ($p < 0.001$, $r^2 = 0.75$). *E. camaldulensis* therefore used both groundwater and vadose zone moisture sources, depending on soil water availability. Model results suggest that groundwater sources represented ~67% of total annual water use.

Citation: Engel, V., E. G. Jobbágy, M. Stieglitz, M. Williams, and R. B. Jackson (2005), Hydrological consequences of Eucalyptus afforestation in the Argentine Pampas, *Water Resour. Res.*, *41*, W10409, doi:10.1029/2004WR003761.

1. Introduction

[2] Grasslands are being converted to plantations and woodlands around the world at an accelerating rate [*Herron et al.*, 2002; *Jackson et al.*, 2002]. Trees generally use more water than cooccurring herbaceous species, and the establishment of plantations in grasslands is therefore likely to alter local hydrology. The consequences of large-scale afforestation on hydrologic cycles depend on factors such as the seasonality of precipitation and evaporative demand, growing season length, soil texture (influencing moisture retention and transmissivity), and management practices [*Williams*, 1990; *Mather*, 1993; *Richardson*, 1998; *Vertessy et al.*, 2000; *Jobbágy and Jackson*, 2004; *McElrone et al.*, 2004]. Increased rainfall interception and transpiration, declines in soil moisture, and decreased stream discharge have all been documented after plantation establishment in various areas [*Calder et al.*, 1993; *LeMaitre et al.*, 1999; *Jackson et al.*, 2001; *Gyenge et al.*, 2002; *Farley et al.*, 2005]. Deep-rooted or phreatophytic plantation species have also been shown to lower groundwater tables [*Bari and Schofield*, 1992; *Cramer et al.*, 1999]. In semiarid and arid regions where the interaction of saline groundwater with upper soil layers is harmful to crop species, the drawdown of water tables by large-scale afforestation can be beneficial. However, in areas characterized by low topographic relief, excessive groundwater use has also been shown to reverse hydraulic gradients belowground, causing localized aquifer discharge in upland plantation root zones [*Heuperman*, 1999; *Jobbágy and Jackson*, 2004].

[3] The Rio de la Plata Grasslands of Argentina and Uruguay provide an ideal system in which to examine the hydrological consequences of vegetation change. Originally treeless, this region hosts one of the largest uncultivated grassland systems in the world [*Soriano*, 1991]. These grasslands also provide an extensive gradient in precipitation, soil chemistry, and soil texture that can be used to test general mechanisms of interactions between hydrologic cycles, biogeochemistry, and vegetation [e.g., *Jobbágy and Jackson*, 2003]. Moreover, in recent decades increasing areas of the Pampas have been converted to plantations, with new provincial and federal tax incentives likely to increase rates of land use conversions further [*Wright et al.*, 2000].

[4] The potential hydrologic and ecological consequences of afforestation in South America are extensive [*Jobbágy*, 2002; *Jobbágy and Jackson*, 2004]. Preliminary observations indicate that plantations of *Eucalyptus camaldulensis* (a phreatophytic species commonly grown in the region) often cause localized drawdowns of water tables and a net flux of shallow, saline groundwater from surrounding grasslands or relatively deep in the soil [*Jobbágy and Jackson*, 2004]. These fluxes appear necessary to support the transpiration demand of *E. camaldulensis* during dry periods, and indicate a significant departure from the regional hydrologic equilibrium that formed with the native grassland species. The higher transpiration rates of *E. camaldulensis* may also cause an increase in salt concentrations

[1] National Park Service, Everglades National Park, Homestead, Florida, USA.
[2] Grupo de Estudios Ambientales, Instituto de Matemática Aplicada San Luis, Universidad de Nacional de San Luis, San Luis, Argentina.
[3] Consejo Nacional de Investigaciones Científicas y Técnicas, Instituto Nacional de Tecnologia Agropecuaria San Luis, San Luis, Argentina.
[4] School of Civil and Environmental Engineering and School of Earth and Atmospheric Sciences, Georgia Institute of Technology, Atlanta, Georgia, USA.
[5] Institute of Atmospheric and Environmental Sciences, University of Edinburgh, Edinburgh, UK.
[6] Nicholas School of the Environment and Earth Sciences, Duke University, Durham, North Carolina, USA.

0043-1397/05/2004WR003761

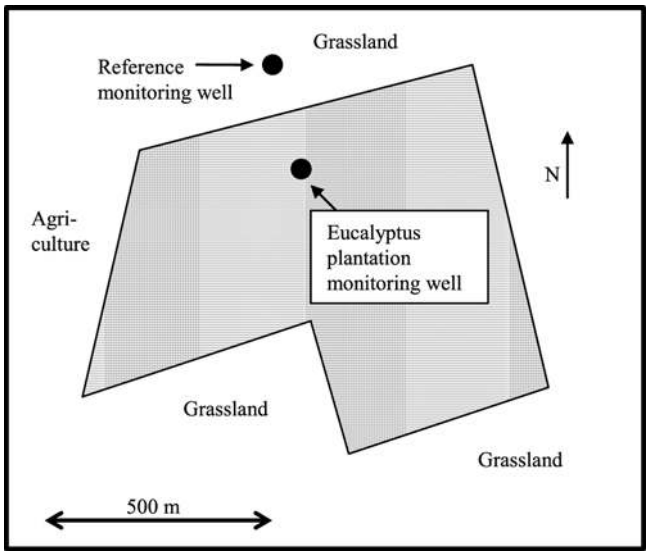

Figure 1. Schematic diagram of *Eucalyptus camaldulensis* plantation in the Flooding Pampas grassland region of central Argentina, located near Castelli, Buenos Aires (36°02.0′S, 57°50.3′W). The grassland reference and plantation groundwater monitoring wells are located 100 m from the grassland-plantation boundary.

belowground through root exclusion during uptake [*Jobbágy and Jackson*, 2003, 2004]. Such changes in soil chemistry accompanying afforestation may ultimately lower the long-term productivity of planted areas [*Cramer and Hobbs*, 1992; *Heuperman*, 1999].

[5] In this study, we use a novel combination of sap flow measurements, local hydraulic gradients, diurnal water table fluctuations, and soil moisture measurements to determine water use characteristics of a *Eucalyptus camaldulensis* plantation established in a native grassland of the Pampas. Groundwater contributions to total sap flow in the plantation are derived from diurnal water table fluctuations and linked with vadose zone moisture content. These observations over 2 years of measurements are then used to validate a detailed soil and canopy soil model for simulating the annual hydrologic mass balance, including unmeasured components such as soil evaporation and groundwater inputs from the surrounding grassland. Model sensitivity analyses provide a context for investigating the biological and physical controls on water balance in the plantation.

2. Methods

2.1. Study Site

[6] The Flooding Pampas, a subset of the much larger Pampas region, are temperate subhumid grasslands occupying ~90,000 km^2 in central Argentina [*Soriano*, 1991]. The climate is temperate: humid, with mean annual temperatures of ~14°C and a mean precipitation rate of ~1000 mm yr^{-1}. The region is extremely flat with slopes of <0.1%. Poor drainage and generally humid conditions determine the presence of a shallow unconfined aquifer in most of the region ranging from <1 to ~10 m below the surface and varying seasonally with the balance of precipitation and evaporative demand [*Tricart*, 1973]. Soils are derived from Quaternary and Holocene loess deposits [*Zárate*, 2003]. Saline/sodic soils with electrical conductivities up to 15 dS m^{-1} are frequent in areas of groundwater discharge [*Soriano*, 1991], whereas nonsodic mollisols occupy recharge zones.

[7] The study described here was performed in a 40 ha *Eucalyptus camaldulensis* plantation at Castelli (Figure 1). The plantation (36°02.0′S, 57°50.3′W) was established in 1951 at 6 m^2 spacing without active management including fertilization or irrigation. It has a current density of 500–700 stems ha^{-1} with a mean tree height ~45 m. The understory is sparse and dominated by the native shrub *Celtis tala*. Herbaceous species in the understory are generally absent except in tree fall gaps.

[8] The surrounding native grassland grows year-round with a mixture of C3 and C4 grasses typical of upland communities in the Flooding Pampas [*Perelman et al.*, 2001]. Average annual precipitation from 1950 to 2002 was 987 mm distributed relatively evenly throughout the year. The soil at the site is a Hapludoll over laying an older eroded soil (II horizons). The horizon sequence at the site is: A (0–15 cm), AC (15–35 cm), IIB (35–75 cm), and IIC (75–300 cm). Surface layers have silty loam textures, with clay content peaking in the B horizon and decreasing at depth. Sediment cores from the area show the presence of silty materials 8 to 10 m below the surface, followed by coarser sediments in contact with a clay layer at 18–20 m [*Servicio Provincial de Agua Potable y Saneamiento Rural*, 1987]. During our study period, the water table was typically located 1–3 m below the surface. Saturated hydraulic conductivity (K_{sat}) in grassland surface soil layers determined from 4 m well tests during September 2002 and January 2003 was 1.0 ± 0.12 m d^{-1} [*Amoozegar and Warrick*, 1986]. Maximum grassland rooting depths are 1–2 m, whereas plantation roots reach 5–6 m depth and coincide with the upper boundary of a fully reduced (gley) sediment layer [*Jobbágy and Jackson*, 2004].

2.2. Stand Characteristics

[9] At three locations (50, 100, and 150 m from plantation boundary) the diameter at breast height (DBH) was measured on 133 mature trees. Measurements of DBH were converted to basal area and divided into four size classes (0–39, 40–49, 50–59, and 60+ cm). Two incremental cores were taken on a subset of 40 trees across all size classes, and the depth of active xylem was estimated visually to the nearest 0.5 mm. The sapwood to basal area ratio did not vary significantly between size classes and a single relationship based on linear regression was used to determine the total sapwood area for all trees in each class (m = 0.18, r^2 = 0.9, $p < 0.001$). To estimate the sapwood area index (SAI, m^2 active xylem m^{-2} ground area), live, dead and missing stems were counted along two adjacent planting rows at the three locations until 20 live trees were encountered. The original planting density of 1 tree per 6 m^2 was converted to the current spacing (1 tree per 19 m^2) using the measured ratio of live trees to dead or missing trees along a planting row (0.32), and was then multiplied by the number of trees measured for DBH (133) to determine the total sampling area. For each size class, the combined sapwood area for all trees in that class was then divided by the total sampling area to determine its fractional SAI. (Table 1).

Table 1. Size Class Distribution and Sapwood Area Index of Sample Trees[a]

Size Class DBH, cm^2	n	Sapwood Area, cm^2	Fractional Area	Size Class SAI, $m^2\ m^{-2}$
0–39	78	10,802	0.334	4.27 E-4
40–49	27	7,844	0.243	3.10 E-4
50–59	21	8,672	0.269	3.43 E-4
60–69	8	4,980	0.154	1.97 E-4

[a]Total sapwood area is 32,298 cm^2. Total sampling area is 2527 m. Site-wide SAI is 1.28×10^{-3} $m^2\ m^{-2}$. Read 4.27 E-4 as 4.27×10^{-4}. DBH, diameter at breast height; SAI, sapwood area index.

2.3. Hydrologic Setting

[10] Water table depths (z) were measured using pressure transducers (model PS9800, Instrumentation Northwest) in two 5 m hand-augured wells installed in the plantation and the adjacent grassland, with both wells 100 m from the plantation boundary. Additional z measurements were taken for shorter periods in the plantation 50 m from the boundary. After correcting for elevation (<3 mm resolution), measurements showed a decrease in potentiometric surfaces from 0.2 to 0.6 m moving from the grassland to plantation (Figure 2). Hydraulic gradients between the grassland and forest disappeared only during very wet periods, occurring twice since observations at the site began in 2001 [*Jobbágy and Jackson*, 2004]. Groundwater levels beneath the plantation during the current study reached their lowest levels between early February and late March 2003 (Figure 2) corresponding with maximum grassland-forest hydraulic gradients. The lowest soil volumetric moisture contents (θ, 0–18 cm, CS615 Campbell Scientific Inc., Logan, Utah) measured at two locations in the plantation 100 m from the grassland edge also occurred during this period, with values closer to field saturation occurring during the winter months. Surface θ in the grassland is typically close to field capacity except during the summer.

2.4. Plantation Water Use: Sap Flow Measurements

[11] For the period August 2002 to May 2003, Granier-type heat dissipation sap flow sensors [*Granier*, 1987; *Phillips et al.*, 1996] were installed in 18 sample trees distributed among the four size classes. One sensor per tree was installed. The 2 cm heated and reference probes were

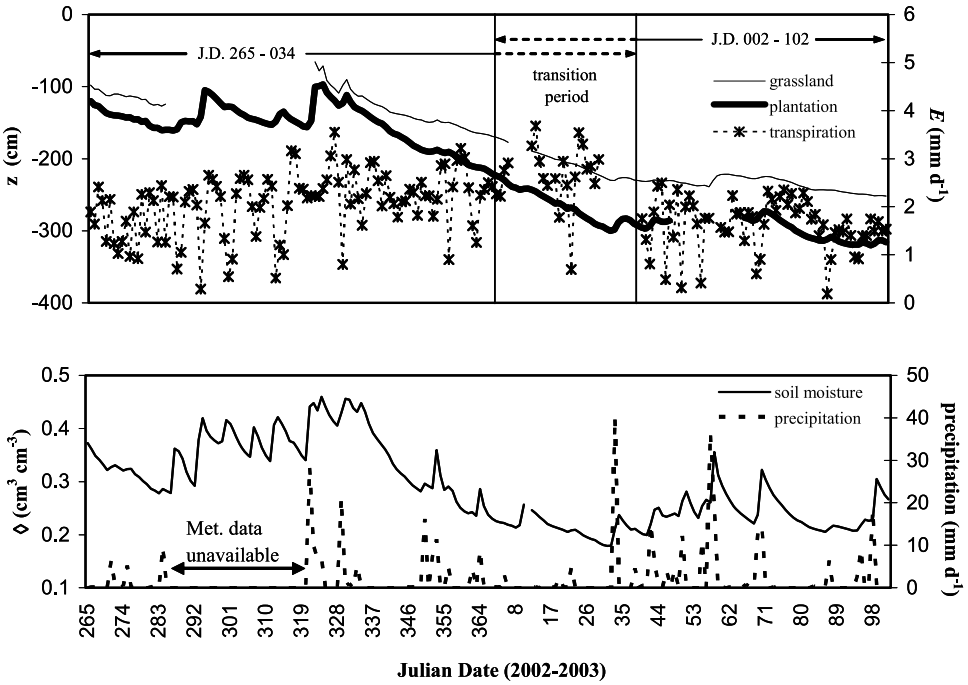

Figure 2. Groundwater, surface soil moisture, and transpiration data from late winter 2002 to late summer 2003 (Julian days (JD) 265–102), divided into two overlapping periods on the basis of the contributions of vadose zone versus deep groundwater to transpiration fluxes. The first period (JD 265–002) is characterized (top) by relatively stable plantation water table depths z ranging from −100 to −200 cm, increasing transpiration (E) associated with seasonal solar inputs, and (bottom) by high surface soil moisture content (θ). The majority of water utilized for transpiration by *E. camaldulensis* during this period is derived from the vadose zone. During a transition period (JD 002–034), surface θ declines to a minimum as evaporative demand reaches maximum values during peak summer conditions. Deep groundwater becomes an increasingly important water source for *E. camaldulensis* during this interval. The mid to late summer (JD 034–102) in the region is characterized by deeper but relatively stable groundwater levels with plantation z fluctuating around −300 cm, recovering θ, and decreasing E associated with declining temperatures and solar inputs. During this period, transpiration rates are independent of surface soil moisture content, and *E. camaldulensis* behaves as a strict phreatophyte (see section 3).

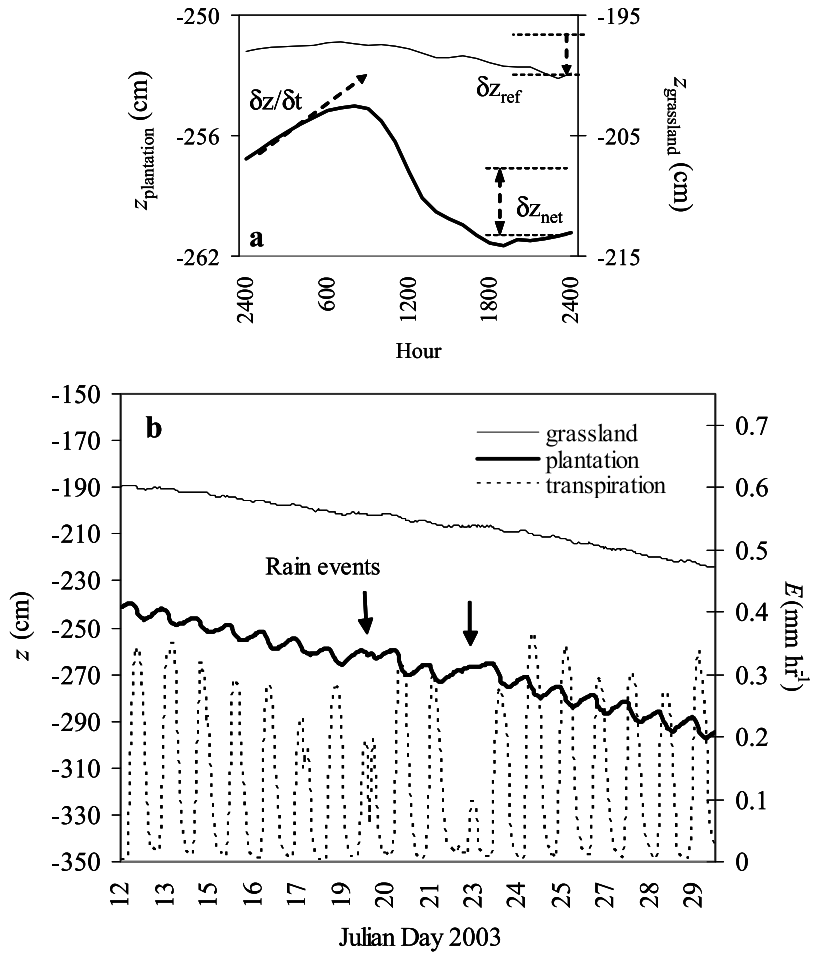

Figure 3. (a) Graphical representation of the components of diurnal water table fluctuations in the plantation and surrounding grassland over a 24-hour period. These terms are combined in equation (3) (see section 2) and used to estimate direct groundwater withdrawals by the plantation. (b) Diurnal sap flow values in *E. camaldulensis* and groundwater fluctuations beneath the plantation are closely correlated over a 2 week period. The legend in Figure 3b applies to both plots.

installed using a low speed drill at a height of 1.5 to 2 m and separated by a distance of ~15 cm. The heated probe and support circuitry were designed to dissipate a constant 0.2W into active xylem. Temperature differentials between the heated and reference probes were measured every 10 s, and 30 min averages were recorded with automatic dataloggers (models CR10X and CR21X, Campbell Scientific Inc., Logan, Utah). Sap flux density (U, kg H_2O m^{-2} sapwood area s^{-1}) in each tree was calculated as

$$U = 0.119\left((dT_{max} - dT)/dT\right)^{1.23} \quad (1)$$

where dT_{max} is the maximum temperature difference recorded during no-flow (predawn) conditions, and dT is the 30 min. average temperature difference between the sensors during positive sap flow conditions [*Granier et al.*, 1990]. Temperature differentials were corrected for the proportion of the heated probe in contact with active xylem after *Clearwater et al.* [1999]. This correction is necessary if the active xylem depth is less than the probe length (2 cm) and this occurred in only 3 of 18 trees.

[12] Stand-level transpiration (E, kg H_20 m^{-2} ground area s^{-1}) was calculated from sap flux density and stand characteristics as

$$E = \sum_{i=1,4} \rho_i U_{avg,i} \quad (2)$$

where ρ is the sapwood area index and U_{avg} is the average sapflux density in each size class i. The 30 min. interval sap flow data were summed over each 24 hr period to give daily total water use in mm d^{-1}.

2.5. Plantation Water Use: Groundwater Fluctuations

[13] During periods of high E and low θ, groundwater levels beneath the plantation fluctuate on a diurnal cycle with amplitudes ranging up to 15 cm (Figure 3). Groundwater fluctuations have been used to quantify transpiration for some time [*White*, 1932; *Freeze and Cherry*, 1986; *Farrington et al.*, 1990], and we apply a modification of traditional techniques for this study. Our method is similar to that of *Salama et al.* [1994], incorporating a hydrologic mass balance approach and a hydrograph separation technique to quantify the sources and sinks affecting plantation z. In this

Table 2. ANOVA Analysis of Laboratory Measurements of Aquifer Specific Yield Calculated Over Three Wetting and Three Drying Cycles[a]

Test	Soil Column 1	Soil Column 2	Column Average
Drying 1	0.0373	0.0368	0.0371
Drying 2	0.0382	0.0379	0.0381
Drying 3	0.0316	0.0380	0.0348
Wetting 1	0.0361	0.0354	0.0358
Wetting 2	0.0321	0.0369	0.0345
Wetting 3	0.0344	0.0366	0.0355
Average drying	0.0357	0.0376	0.0366
Average wetting	0.0342	0.0363	0.0353
Average of all tests	0.0350	0.0369	0.0359

[a]The p value between soil columns is 0.0726, and the p value between cycles is 0.1523.

approach, direct withdrawals from groundwater through transpiration (E_{gw}, mm d^{-1}) are calculated as

$$E_{gw} = \left(24\delta z/\delta t - \delta z_{ref} + \delta z_{pl}\right)*SY \quad (3)$$

where $\delta z/\delta t$ is the rate of increase in groundwater levels (mm hr^{-1}) from 0 to 4 a.m. multiplied by 24 to estimate inputs from the shallow aquifer in the surrounding grassland (Darcian flow), δz_{ref} represents regional groundwater fluctuations not associated with local influences and is estimated from net daily changes (mm d^{-1}) in the reference monitoring well in the grassland, δz_{pl} is the net change in plantation z (mm) over a 24 hr period, and SY is the aquifer specific yield (m mm^{-1}). A graphical representation of the component terms in equation (3) over a 24 hr cycle is displayed in Figure 3.

[14] On a daily basis, transpiration measured by sap flow (E) should equal groundwater use (E_{gw}) plus changes in vadose zone soil moisture (δSM). Combining equations (2) and (3) and adding the soil moisture term gives

$$\delta z = 1/SY(E - \delta SM) \quad (4)$$

where δz is the sum of fluxes contributing to the diurnal groundwater fluctuations ($24\delta z/\delta t - \delta z_{ref} + \delta z_{pl}$). Applying a simple linear regression through values of δz (x axis) and E (y axis) yields a relationship between δz and E such that the inverse slope should equal the specific yield SY of the aquifer. Equation (4) was also used to solve for soil moisture contributions to E during periods when the correlation between E and δz was poor. Days with precipitation events were excluded from this analysis.

[15] Equation (4) was also used to determine transpiration withdrawals from the vadose zone. Since $E_{gw} = \delta z*SY$, equation (4) can be rearranged to show that the term δSM is equivalent to $E - E_{gw}$. The fraction of total transpiration withdrawals derived from the vadose zone therefore follows as $(E - E_{gw})/E$.

2.6. Specific Yield Laboratory Measurements

[16] As an independent estimate of SY, laboratory measurements were performed on intact soil cores. For an unconfined aquifer, SY can be defined as the ratio of a measured change in z to the actual amount of water added to or removed from the water table. SY represents the water storage capacity of the saturated soil per unit depth [*Morris and Collopy*, 1999] or alternatively, the difference between total porosity and field capacity per unit volume of soil. Typical values range from 0.2 to 0.3 for sandy materials to <0.05 for soils with higher clay content. Hysteresis and air entrapment effects may lower these values by as much as one half in systems with fluctuating water levels. For this reason we performed SY laboratory measurements under fluctuating conditions similar to those observed in the field.

[17] We obtained two intact soil columns (72 and 85 cm lengths) in May 2003 from the forest interior 50 m from the grassland transition. PVC pipes (id 104 mm) were hammered directly into the soil starting at −2 m from the bottom of a soil pit. In the laboratory the columns were aligned vertically and connected through the bottom to an elevated water source equipped with a pass valve. A 12 mm id core was taken from the center of each soil column to 15 cm above the bottom. The soil column was saturated by opening the pass valve until the water level in the center well was 2–3 cm below the surface. The valve was then closed and the column was subjected to surface drying with directed airflow. The intensity of drying was regulated to generate water table depressions of 16–19 cm in 10–12 hours. Changes in soil column water content during the drying cycle were determined gravimetrically. Water table depths were measured in the wells with a floating element and thin ruler. The dried columns were later subject to a rewetting cycle to create a water level rise of 16–19 cm in 12–14 hours. Water consumption was measured by controlling additions to the elevated source using a graduated cylinder. Three full wetting and drying cycles were repeated on the two soil columns. Water volumes entering or leaving the source chamber were corrected for the amount of water contained in the observation well to determine changes in soil water storage. These storage values were divided by the corresponding changes in water table depths to obtain a value for SY (Table 2). This value was used to parameterize the physical properties of the soil column model for simulations of groundwater dynamics beneath the plantation.

2.7. Model Description

[18] A brief description of the model structure is presented here and in more detail in Appendix A. A more complete description is given by *Williams et al.* [1996, 2001] and *Engel et al.* [2002]. Direct measurements for baseline model parameter values were used when available (Table 3). For the canopy model parameters not measured on site, literature values or reasonable estimates were used from simulations in other temperate forested systems [*Williams et al.*, 1996; *Engel et al.*, 2002]. Hourly meteorological input data were measured on a 3 m tower established in the grassland 100 m from the plantation edge and included precipitation, air temperature, relative humidity (CS 500, Campbell Scientific, Logan, Utah), and wind speed (Model 014A, Campbell Scientific, Logan, Utah). Longwave radiation inputs to the model were converted from air temperature minus 20 K and the Stefan-Boltzmann formulation [*Jones*, 1992]. Meteorological conditions at the site were monitored for 18 months beginning in August 2002 and were used to drive the model simulations. In October and November 2002, rainfall measurements were lost briefly because of equipment malfunction. Precipitation amounts

Table 3. Simulation Model Baseline Parameter Values

Model Parameter	Value				
Minimum leaf water potential Ψ, MPa	−2.7				
Leaf area index LAI, $m^2\ m^{-2}$	4.25				
Canopy height, m	45				
Rooting depth, m	6				
Fine root resisitivity, MPa s m $mmol^{-1}$	200				
Total fine root biomass, g m^{-2}	3500				
	Soil Layer				
	1	2	3	4	5
Mineral classification	sandy loam	clay	silty loam	silty loam	silty loam
Thickness, m	0.4	0.5	0.6	2.0	2.5
Hydraulic conductivity, m s^{-1}	1.0 E-5	1.6 E-7	1.0E-5	7.5 E-6	5.0 E-6
Root biomass density, kg m^{-3}	0.7	0.1	0.6	0.6	0.5

and timing during this period were estimated from surface soil moisture changes in the grassland.

[19] The model subroutines governing soil column processes were modified from *Stieglitz et al.* [1997] and *Engel et al.* [2002]. The primary modifications included the addition of routines for simulating capillary action above the free water surface. In this scheme, capillary transport moves water from saturated zones upward to soil layers with a matric potential less than the equilibrium value based on elevation above z. In saturated layers the matric potential was added to a constant (−0.36 MPa) osmotic potential term. This value is based on electrical conductivity (EC) measurements of groundwater at the site that averaged 10 mS m^{-1} [*Jobbágy and Jackson*, 2004].

[20] Model results were calibrated on both hourly and daily timescales against transpiration and groundwater measurements collected between December 2002 and April 2003. Modeled daily hydrologic fluxes were integrated to give annual values covering the period December 2002 to December 2003, and included external groundwater inputs and the fraction of total transpiration source water in the plantation derived from saturated zones.

3. Results

3.1. Plantation Water Use, Soil Moisture, and Groundwater Fluctuations

[21] Sap flow derived transpiration rates (E) averaged ~2 mm d^{-1} over the study period with maximum rates of ~3.7 mm d^{-1} (Figure 2). Total daily transpiration rates were closely correlated with both total solar radiation ($r^2 = 0.75$; $p < 0.001$) and daily average bulk atmospheric VPD ($r^2 = 0.70$; $p < 0.001$). Comparing daily E to Penman potential evapotranspiration (PET) indicated seasonal water stress during the summer decrease in surface soil moisture (θ), with the ratio E:PET decreasing to low values (~0.4) during this period (data not shown). Ratios of E: PET increased in the fall and winter periods, averaging ~0.6 and were correlated with cooler temperatures and increasing precipitation at the plantation.

[22] During periods of high E and low θ in the summer dry season, groundwater levels beneath the plantation fluctuated with daily amplitudes of up to 15 cm (Figure 3; fluctuations uncorrected for specific yield). Decreasing groundwater levels during the day corresponded with direct transpirational uptake by *Eucalyptus* roots, while increasing groundwater levels at night were likely due to Darcian flow or upwelling of deeper sources caused by the hydraulic pressure of the shallower aquifer in the surrounding grasslands (Figure 3). Rainfall events tended to raise overall groundwater levels due to recharge and to reduce transpiration withdrawals by lowering evaporative demand at the leaf surface (Figure 3). On days without rain, fluctuations in z on hourly timescales closely tracked sap flow-derived estimates of E. However, the relationship between net daily groundwater fluctuations (δz) and stand transpiration E measured as sap flow also varied seasonally (Figure 4, top). For example, values of δz and E in summer to early autumn (JD 002–102) showed a close correlation, while the relationship between these variables during winter and spring (JD 265–002) was weaker. The correlation between E and δz during the summer and early autumn suggests a significant groundwater contribution to total *Eucalyptus* water use during this period, with a low and relatively constant contribution from soil moisture.

[23] An estimate of the sediment specific yield (SY) (equation (3)) was necessary to convert net daily groundwater fluctuations (δz) to transpiration withdrawals (E_{gw}), and two independent methods converged on the same estimate for this system. Linear regression through the points in Figure 4 (top) collected during periods of low surface soil moisture yielded a value for SY of 0.038 ± 0.004 m mm^{-1} ($p < 0.001$; equation (4)). This value showed close agreement with the average value of 0.0359 m mm^{-1} determined from independent soil column laboratory measurements (Table 2). In the regression method, the y intercept (13.7 ± 6.4 mm d^{-1}; $p = 0.05$) may represent fluctuations in z owing to other physical processes (e.g., changes in air pressure) or to error in estimates of transpiration at low sap flow rates.

[24] Measurements of groundwater and θ suggest that *E. camaldulensis* derived transpiration source water from both saturated and unsaturated zones during periods when θ was high (JD 265–002) but gradually shifted to strict phreatophytic behavior during a transition period (JD 002–034) as θ declined to minimum values (Figure 4). Prior to this shift, during JD 265–002, soil moisture in the unsaturated zone contributed significantly to E and caused inconsistent relationships between E and δz (Figure 4, top, squares). Residual analysis (Figure 4, bottom) indicates that during this period the differences between observed and regression-predicted δz decreased with θ ($r^2 = 0.75$; $p < 0.001$). This

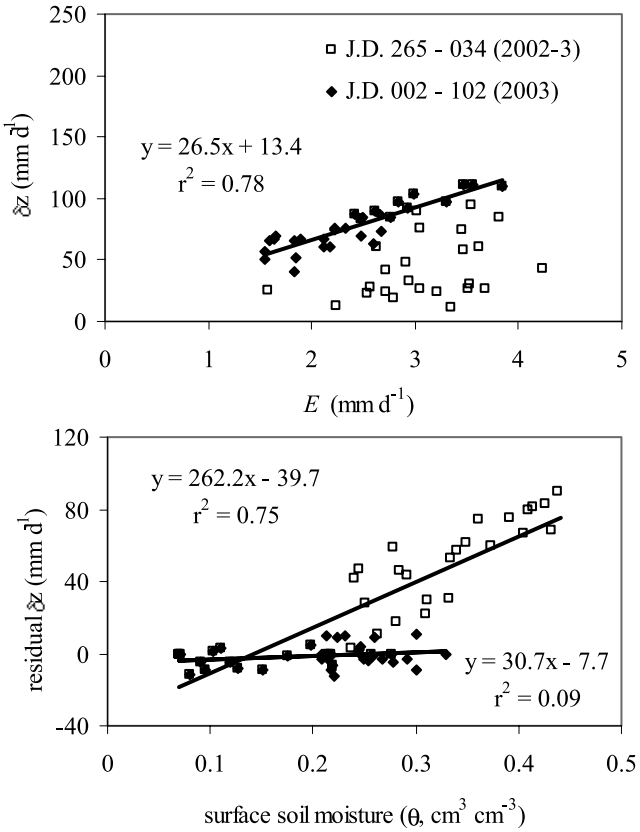

Figure 4. (top) Relationship between δz (equation (3), an indicator of direct groundwater use) and total transpiration E derived from sap flow measurements during periods of high (JD 265–034, squares) and low (JD 002–102, diamonds) surface soil moisture conditions. Overlapping points occurred during the transition period (JD 002–034; see Figure 2). The inverse slope of the regression in Figure 4 (top) represents the specific yield (SY) of the plantation soils. (bottom) Deviation from regression line in Figure 4 (top), shown to be a function of soil moisture during wetter periods (squares). During the second half of the simulation period with drier conditions (diamonds) residual values are unrelated to surface soil moisture.

relationship therefore suggests that *E. camaldulensis* functions as a facultative phreatophyte – increasingly withdrawing water from saturated zones as vadose zone θ declines seasonally. The results in Figure 4 (bottom) also show that following the decrease of θ to an apparent threshold level of $\sim$0.15 cm^3 cm^{-3} between JD 002 and 034, the relationship between E and δz thereafter became largely independent of θ. This is apparent from the weak correlation (r^2 = 0.09) between residual δz and θ after this period and the days following up to JD 102. During this interval, residual δz values were small and did not increase as θ values increased to $\sim$0.3 cm^3 cm^{-3} with rain events near end of the sampling period. During this time the trees continued to function as strict phreatophytes deriving the majority of transpiration water from saturated zones.

[25] The switch from facultative to strict phreatophytic behavior by *E. camaldulensis* in the summer caused a seasonal change in the relationship between plantation water table depths (z) and groundwater withdrawals (Figure 5). For example, during the spring and early summer between JD 265–002, θ decreased (Figure 3) and net groundwater withdrawals (δz) by *E. camaldulensis* gradually increased (Figure 4). As δz increased during this period, the depth to the water table also increased (Figure 5, squares). However, during mid to late summer and fall (JD 034–102) δz and E both decreased and θ began to increase, while z did not recover but instead continued to decline below −300 cm (Figure 5, diamonds). The lack of recovery in z indicates that the proportion of total transpiration derived from beneath the water table by these trees remained high after seasonal reductions in E. The switch to strict phreatophytic behavior by *E. camaldulensis* during the summer and early fall therefore changed the relationship between water table depth and transpiration rates in the plantation. The continued decline in z in the fall indicates that although groundwater withdrawals by the plantation were decreasing during this period, these withdrawals remained greater than the net flux of groundwater into the plantation.

3.2. Vadose Zone Contributions to Plantation Water Use

[26] Our observations of θ, sap flow, and θz were also used to estimate transpiration withdrawals from the vadose zone during days when the correlation between E and δz was poor (equation (4)). A lack of correspondence between E and δz was observed primarily during the period between JD 265 and 034. During this period, our observations showed that the proportion of vadose zone moisture supplying transpiration increased to $\sim$100% as θ approached $\sim$0.45 cm^3 cm^{-3} in the upper soil layers (Figure 6). A third-order polynomial produced the best fit between observations of θ and the estimated withdrawals from the vadose

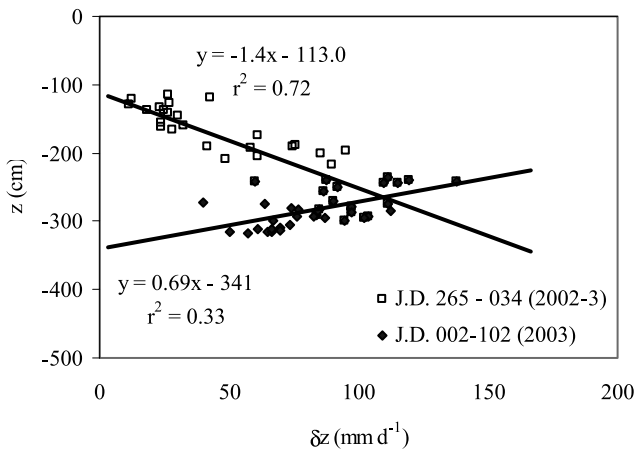

Figure 5. Daily groundwater withdrawals δz (uncorrected for SY) through transpiration uptake show a seasonally changing relationship with water table depth z. Increasing δz values cause declining z over the initial portion of the study period (JD 265–034). Later in the study period, z declines further despite decreasing δz and decreasing transpiration withdrawals. A decrease in hydraulic conductivity below −250 cm may limit Darcian flow from the surrounding grassland, causing continued decreases in z despite the lower transpiration rates and maximum grassland-plantation hydraulic gradients during this part of the year.

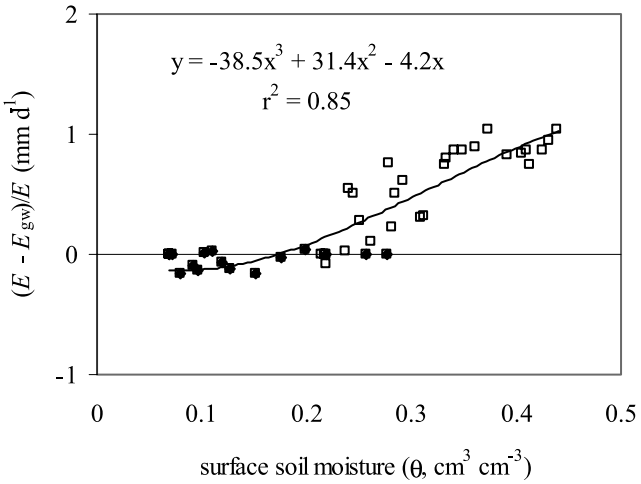

Figure 6. Fraction of transpiration withdrawals derived from the vadose zone (based on the difference between total sap flow E and direct groundwater uptake E_{gw}), which increases asymptotically to 1 as surface soil moisture values approach 0.45 cm^3 cm^{-3}. Negative fractions on the y axis are likely the result of measurement error causing transpiration rates derived from δz to be higher than derivations from sap flow measurements. The majority of the negative values represent data collected during the transition period. The slope of a line fit through the transition period data (solid symbols) is not significantly different from zero ($r^2 = 0.17$; $p = 0.23$).

zone and suggests the fraction of total transpiration water derived from unsaturated zones exhibits a positive sigmoidal relationship with θ.

3.3. Model Simulations

[27] The diurnal fluctuations in plantation water table depths observed during the late spring and summer are reproduced well in the model results (Figure 7a). Over the 1 year simulation period, modeled, daily average z exhibited a mean bias of +0.05 m compared to observations with a root mean square error of 0.16 m. Modeled hourly transpiration rates also show close agreement with measured values (Figure 7b; $r^2 = 0.85$; $p < 0.001$). Overall, the model results compared well with observations and suggested that the biophysical factors controlling root uptake and groundwater levels were represented reasonably in these simulations.

[28] The modeled annual hydrologic mass balance suggests that ~67% of transpiration source water came directly from groundwater (Table 4). Closer inspection of model results reveals this percentage to change seasonally, with values generally increasing as water tables begin to decline during the wet-dry season transition period. Integration of daily results over the 1 year simulation period showed the amount of groundwater lost to deep drainage beneath the plantation (621 mm) and the Darcian inflows from the surrounding grassland (698 mm) were of similar magnitude as precipitation (804 mm) and transpiration (592 mm). This balance suggests that while the high plantation E accounted for deeper water tables and the local hydraulic reversals with respect to the topographically lower grasslands, seasonal groundwater levels at this site were also controlled to a large extent by regional hydrologic fluxes. Modeled soil evaporation rates represented ~14% of total evapotranspiration in the system. Direct groundwater uptake through roots was estimated at 395 mm yr^{-1} (Table 4).

[29] A series of simulations was used to test the sensitivity of transpiration and other components of the plantation water budget to changes in model parameters controlling hydrologic processes (Table 4). These simulations showed that annual E was more sensitive to model parameters governing evaporative demand at the leaf surface than parameters governing root uptake. For example, increasing LAI by ~50% from baseline values resulted in a 30% increase in annual E, while lowering the value of midday leaf water potential (Ψ_L) causing full stomatal closure by ~25% resulted in a 38% increase in E. On the other hand, increasing root biomass by 50% from baseline values resulted in only a 3% increase in E (results not shown). In all cases, the amount of groundwater transferred through Darcian flow from the grassland to the plantation was positively correlated with E. In the simulations with E reduced below baseline values, Darcian inputs remained greater than the amount of water lost to deep drainage and the plantation continued to function in these runs as a net groundwater discharge zone for the surrounding grassland.

[30] With one exception, total annual inputs (precipitation plus Darcian flow) were greater than total losses (evapotranspiration, surface runoff, and deep drainage) in these simulations, and caused a net annual increase in total soil column water storage beneath plantation. The modeled increases in soil storage were due in part to the simulation interval (December 2002–December 2003) over which

Table 4. Modeled Baseline Hydrologic Water Budget for the Plantation and Sensitivity Analysis of Model Parameters[a]

Precipitation	Thrufall	Wet Canopy Evaporation	Eucalypt Transpiration	Soil Evaporation	Groundwater Withdrawals	Darcian Inputs From Grassland	Deep Drainage	Surface Runoff	Change in Soil Moisture	Simulation[b]
803	677	125	592	118	395	698	621	10	34	1
803	634	163	770	106	504	897	621	9	30	2
803	729	73	348	139	237	443	622	16	48	3
803	677	125	607	117	120	157	621	10	−521	4
803	677	125	592	118	400	691	621	10	27	5
803	677	125	420	124	288	542	621	10	44	6
803	677	125	817	108	529	904	622	10	24	7

[a]All values are in mm yr^{-1}.
[b]1, baseline model simulation with calibrated parameter values; 2, LAI = 6.25; 3, LAI = 2.25; 4, soil hydraulic conductivity = 0.5 (1×10^{-5} m s^{-1}); 5, soil hydraulic conductivity = 2.0 (1×10^{-5} m s^{-1}); 6, minimum $\psi_L = -1.7$ MPa; 7, minimum $\psi_L = -3.7$ MPa.

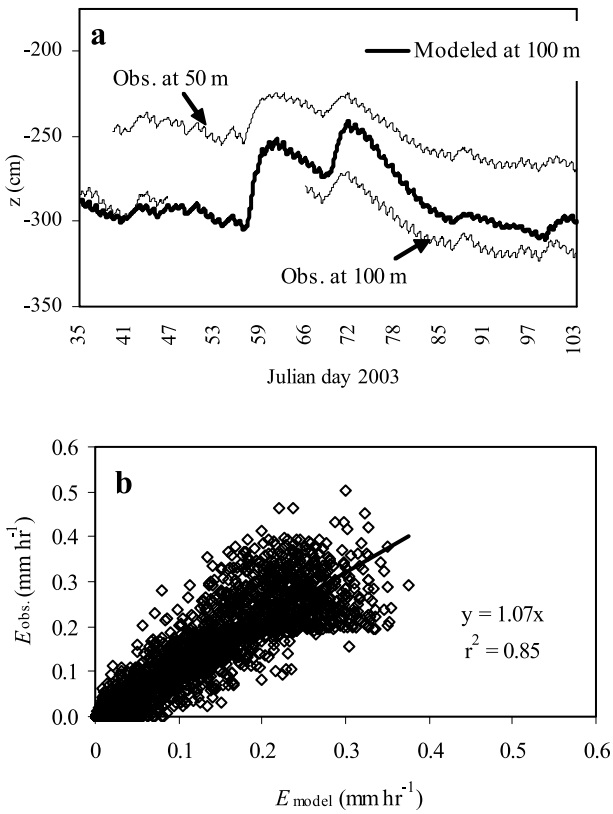

Figure 7. Modeled and observed hourly (a) transpiration rates and (b) groundwater levels beneath the plantation. The model was calibrated to simulate plantation groundwater levels z at 100 m from the grassland edge. Observations of z at 50 m from the grassland edge in Figure 7b are shown for reference.

fluxes were integrated beginning with a relatively dry soil period and ending with a period of significant precipitation and soil recharge. The simulation that showed a net annual decrease in plantation soil water was produced by lowering the value of saturated hydraulic conductivity controlling Darcian inputs from the grassland by 50%. Although only this simulation resulted in a negative annual soil water balance, all of the simulations did show significant seasonal decreases in soil water during the late spring and summer. Interestingly, the simulation with a 50% decrease in saturated hydraulic conductivity also showed a 2.5% increase in E above baseline values. In this simulation, water table depth z was continuously lower than baseline values and decreased to the −6 m model boundary in 167 days. Since saturated layers in the soil column were parameterized with −0.36 MPa osmotic potential, decreases in z caused the integrated osmotic potential of the soil column to increase to 0 MPa at z = −6 m. In this model, E is proportional to the soil−leaf water potential gradient such that higher soil water potential results in lower belowground hydraulic resistance to root uptake. The slight increase in E above baseline values in this simulation therefore resulted from the increase in soil osmotic potential and overall decrease in belowground resistance. Although soil column matric potential also decreased with z and θ in this simulation, the increase in osmotic potential offset these decreases in matric potential and permitted the 2.5% increase in E.

4. Discussion

[31] The combination of well data, sapflow, and vadose zone soil moisture (θ) measurements showed that the study plantation used a significant amount of groundwater, creating a strong hydraulic gradient that drove a nearly continuous water supply from the surrounding grassland area. Our results also indicated that transpiration uptake by *E. camaldulensis* in this plantation was restricted to unsaturated, upper soil layers only when θ approached 0.45 cm^3 cm^{-3}. On the other hand, during the summer when θ was between 0.15 to 0.24 cm^3 cm^{-3}, nearly all transpiration water was derived from deep groundwater sources. Since drier surface conditions are correlated with lower water table depths, groundwater use by *E. camaldulensis* was found to increase with depth to the water table z. Interestingly, during these dry periods the ratio between daily E measured as sapflow and the net groundwater fluctuations (δz; Figure 4) was found to match very closely the specific yield of the sediments (∼0.036 m mm^{-1}) measured in the laboratory.

[32] The sap flow−derived transpiration rates for *E. camaldulensis* measured in this plantation are similar to values reported in other natural and managed stands [*Salama et al.*, 1994; *Cramer et al.*, 1999; *Mahmood et al.*, 2001]. The observed switch from semiphreatophytic to strict phreatophytic behavior by *E. camaldulensis* has also been previously documented in other studies. For example, *Mensforth et al.* [1994] used isotopic tracers and measurements of soil−leaf water potential gradients to investigate uptake zones for a stand of *E. camaldulensis* overlying a saline aquifer, while *Morris and Collopy* [1999] used sap flow and a hydrologic mass balance to determine groundwater withdrawals. In these two studies, *E. camaldulensis* accessed both deep groundwater and vadose zone moisture sources when surface soil layers were relatively wet, but switched to deep groundwater only during drier periods.

[33] Over the 1 year simulation period the calibrated model results suggest that approximately 67% of total transpiration source water was derived directly from groundwater (Table 4). In comparison, *Thorburn and Walker* [1994] found on an annual basis 50−70% of transpiration source water for a stand of *E. camaldulensis* located near an ephemeral stream was derived from groundwater sources. Our modeled estimates of groundwater use by this species are within the range reported in other studies [*Cramer et al.*, 1999; *Morris and Collopy*, 1999].

[34] Higher groundwater use in the plantation relative to the native grassland communities was apparent from the overall lowering of z with respect to surrounding water tables throughout our study (Figure 2). Since the largest grassland-plantation hydraulic gradient (∼0.6 m) occurred at the end of the summer following an extended period of low θ, this suggests the hydrologic impacts of plantations may be most pronounced during drier summer conditions. *Jobbágy and Jackson* [2004] also noted the occurrence of diurnal groundwater fluctuations in this plantation during dry periods that did not occur in the nearby reference wells, indicating increased groundwater access by *E. camaldulensis* relative to the native grasses. This pattern was found to be consistent with the observed difference in maximum rooting depths in the plan-

tation (~6 m) and the surrounding grassland (~1.5 m). Thus, during periods of high evaporative demand and low θ, when transpiration rates in grassland communities are expected to decrease with increasing water stress and senescence, deep-rooted trees such as *Eucalyptus* spp. may have the most impact on local water tables and hydrologic balance.

[35] During the latter portion of the study period, θ increased with several rain events, but the fraction of source water for *E* withdrawn from beneath the water table during and following these events remained high between 60 and 70%. During this interval, total transpiration rates declined from the summer maximum as seasonal temperatures and evaporative demand also decreased. However, the continued high fraction of *E* withdrawn from the saturated soil layers resulted in the continued lowering of *z* despite the increased rainfall and higher water tables in the surrounding grassland. A declining *z* is predicted assuming the sum of transpiration withdrawals plus deep drainage is greater than recharge from the shallow water table (e.g., Darcian flow) in the surrounding grassland ($24\delta z/\delta t$ in equation (1)). Inspection of the component terms defining δz showed Darcian inputs from the surrounding grassland decreased during the latter portion of the study period despite the increasing hydraulic gradient across the two systems reaching maximum values of ~0.6 m. The decreased Darcian inputs may have been due to lower hydraulic conductivities with depth in the soil column restricting flow across the plantation boundary, with the resulting decrease in lateral inflows being insufficient to maintain or raise plantation *z* during the late summer, despite declining *E* and groundwater uptake. In a related study covering other areas of the Pampas, *Jobbágy and Jackson* [2004] showed that the productivity of *E. camaldulensis* decreased in plantations on soils with low hydraulic conductivity and cited increased water stress as a limiting factor in these systems.

[36] The continuation of strict phreatophytic behavior in *E. camaldulensis* during the latter portion of the study period, when precipitation inputs raised surface θ, caused a seasonal hysteresis in the relationship between groundwater uptake, transpiration, and *z* in this plantation (Figure 5). The inability of these trees to utilize surface moisture sources during this period may have been due to root mortality in the upper layers following seasonal drought stress [*Gill and Jackson*, 2000], though the exact mechanism is unknown. Similar preference for saline groundwater compared to fresh surface moisture sources has been noted for *E. camaldulensis* in other studies [*Thorburn and Walker*, 1994; *Mensforth et al.*, 1994]. Grass species, on the other hand, generally respond more quickly to precipitation inputs after dry periods and utilize surface moisture sources to meet transpiration demands [*Soriano*, 1991]. Given this differential response to periodic rain events and the reliance of tree species on groundwater, the large-scale afforestation of Pampas grasslands could result in seasonal changes in water table depths and surface soil moisture content relative to that which occurred naturally with the native grassland vegetation. For example, water table depths may be expected to remain longer at minimum levels in areas of silviculture compared to grassland following the decreases in evaporative demand in the late summer. Such shifts in seasonal groundwater levels may have implications for rainfall-runoff responses and characteristic hydrographs of streams draining this region [*Herron et al.*, 2002; *Farley et al.*, 2005].

4.1. Method Evaluation

[37] The combination of hydrological and ecophysiological approaches used here allowed us to quantify the daily and seasonal relationships between *E*, θ, and *z* (Figures 3–6 and equations (3) and (4)). We adapted techniques originally designed to determine vegetation-induced aquifer discharge in the context of larger-scale hydrologic budgets [*Farrington et al.*, 1990; *Thorburn et al.*, 1993], increasing their temporal resolution (Figure 5) and complementing them with analyses of soil moisture (Figure 6). Additionally, the close agreement between the value of SY derived from lab measurements with the value based on sap flow and groundwater fluctuations suggests a novel approach for using well data as a complement to sap flow to characterize belowground processes (see *Bauer et al.* [2004] for a related application of this method).

[38] Some constraints with the approach presented here need to be considered. For example, the sap flow data confirm δz*SY can be considered as a proxy for *E* only when upper soil layers are dry and not a significant moisture source (Figures 4–6). The method is also limited to periods when groundwater fluctuations due to *E* are dominant with respect to other forcings such as precipitation recharge or air pressure changes [*Salama et al.*, 1994]. Because air pressure effects were not apparent in our grassland monitoring well we did not need to apply corrections for this term. Precipitation events, however, did cause rapid changes in *z*, and data collected on these days were excluded from the analyses. Much of the monitoring well data from the initial study period (JD 265–002) has to be excluded because of the absence of coherent, diurnal groundwater fluctuations. During this period *z* was high and ranged between −100 and −200 cm over weekly timescales with *E* values up to 3.5 mm d^{-1}. Diurnal groundwater fluctuations became apparent only when *z* fell below −150 cm. (Figure 6). The lack of clear fluctuations during much of this interval may simply have been due to a larger fraction of source water being withdrawn from vadose or capillary zones. However, higher hydraulic conductivities in the upper compared to lower soil layers may also have resulted in a more efficient transfer from the surrounding grassland aquifer, thereby preventing significant water table depressions on subdaily timescales. Alternatively, decreased SY in the upper soil layers due to textural changes could have also resulted in less intense fluctuation patterns.

[39] The method of converting sap flux measurements on individual trees to whole-stand water use rates introduced potential errors into our estimates of *E* and the comparisons with δz. Though our overall sample size (n = 18) was large enough to sample multiple trees in each size class, installing more than one sap flux sensor per tree may have improved our estimates of average sap flux velocity and total stand water use. Furthermore, we assumed no variations in sap flux velocity with xylem depth beyond the 2 cm of the probe length. More accurate estimates of *E* would have resulted with the measurements of sap flux velocity at multiple depths within the xylem of the sample trees. Scaling errors associated with variations in radial sap flux velocity are reduced in diffuse-porous species such as *E.*

camaldulensis compared to ring-porous species [*Clearwater et al.*, 1999].

4.2. Modeling

[40] The close correlation between well data and observed transpiration rates with model results (Figure 7) suggests the soil-root-leaf dynamics in this system were reasonably well represented. Modeled z slightly overestimated monitoring well observations at 100 m from the grassland transition but were always less than z recorded at 50 m. Observations of declining z moving toward the plantation center reflect a decreasing ratio of Darcian inputs relative to transpiration withdrawals with distance from the more shallow grassland water tables. Since predicted z at 100 m was shallower than observations at this distance, modeled groundwater inputs from the surrounding grassland may have been overestimated. This model inaccuracy may have resulted from the application of Darcy's law and the coarse 1-D representation of groundwater flux in this system. Heterogeneous sediments or topographic variability between the grassland and plantation monitoring wells may have reduced the suitability of this approach. However, our field observations and multiple core samples at this site showed homogeneous substrate conditions from -1 to -6 m and justified the application of Darcy's law to belowground fluxes in this system.

[41] Model results showed that the groundwater contributions to transpiration (E_{gw}) increased with declining z at the beginning of the summer season, agreeing with observed trends (Figure 4). This increasing reliance on groundwater is a function of the root resistance formulations and the close covariance between surface θ and z in the model structure (Appendix A). For example, declining z in this system is always associated with a drying soil column and increasing hydraulic resistance to root uptake in the vadose zone. As a result, the larger fraction of total belowground resistance was located in unsaturated versus the saturated layers, and a larger proportion of transpiration source water was taken from beneath the deepening water table. Conversely, precipitation inputs and increasing θ in upper soil layers are associated with rising z. Higher hydraulic conductivity and a large percentage of total root biomass in these upper layers results in a lower fraction of transpiration water withdrawn from beneath the shallower water table.

[42] The second part of the simulation period was marked by large grassland-plantation hydraulic gradients increasing up to 0.6 m. To maintain modeled plantation z close to observations during this period, a linear decline in saturated hydraulic conductivity between -1.5 and -6 m soil depth was adopted to reduce Darcian inputs from the surrounding grassland. During this portion of the study period, our observations showed *E. camaldulensis* displayed phreatophytic behavior after the partial recovery of surface θ. Groundwater uptake in the model during this interval, on the other hand, is distributed more to the unsaturated vadose zone. As a result, modeled z does not decline as a function of groundwater uptake during the latter portion of the simulation period as quickly as observations indicate. As discussed above, fine root mortality during the dry season may have been responsible for the continued phreatophytic behavior displayed by *E. camaldulensis* after the seasonal recovery of θ, but temporal root dynamics are not included in the model environment.

[43] *Jobbágy and Jackson* [2004] suggested that root exclusion during groundwater uptake contributed to an observed buildup of salinity beneath this plantation relative to the nearby grassland. Salinity typically increases in zones of net groundwater discharge [*Heuperman*, 1999; *Morris and Collopy*, 1999; *Mahmood et al.*, 2001]. However, the baseline annual water balance presented here (simulation 1 in Table 4) suggested thru fall plus Darcian inputs to the plantation (recharge) were greater than groundwater uptake, deep drainage and soil evaporation (discharge). These model results would not necessarily be expected to cause an increase in salinity beneath the plantation. However, the model results did also indicate an extended period ($\sim$100 days) of net groundwater discharge during the summer as modeled z declined from -100 to -300 cm. This decrease in modeled z matched observations during this period. Incomplete flushing of salts from the root zone after extended periods of net groundwater discharge may be one mechanism responsible for the modeled annual groundwater fluxes presented here and the salinity observations presented by *Jobbágy and Jackson* [2004]. Preferential vertical flow though macropores formed by decaying root has been observed in other *Eucalyptus* plantations [*Bramley et al.*, 2003] and suggests that periods of positive water balance may not remove salt concentrations initiated during uptake. Spatial variability in evapotranspiration excess over precipitation in the plantation [*Calder*, 1998] could also have led to increased plantation groundwater discharge and salinity not captured in the 1-D model framework. Finally, estimates of stand-level transpiration are highly sensitive to the value of LAI used in the simulations; additional LAI measurements elsewhere in the Pampas and at Castelli suggest that the modeled LAI of 4.25 might be low for this system during the summer, leading to an underestimate of E. Higher values of E associated with increased LAI may lead to a negative annual water balance and a buildup of salinity beneath the plantation.

4.3. Controls on Plantation Water Use

[44] The observations and model sensitivity analyses help describe the principal biophysical factors governing plantation interactions with grassland hydrologic cycles. First, observations showed E throughout the study period was almost linearly related to total solar radiation and daily average VPD, indicating water use was controlled primarily by available energy and overall evaporative demand in this system. Concurrent with these results, modeled E was most sensitive to the canopy parameters describing LAI and the minimum midday Ψ_L causing stomatal closure (Table 4). In the model, both of these parameters are primary determinants of total canopy water use, since total evaporating surface area is proportional to LAI, and the minimum Ψ_L sets soil-root-leaf hydraulic limits on water loss at leaf surfaces [*Williams et al.*, 1996]. The strong sensitivity of E to LAI and minimum midday Ψ_L therefore reflects the atmospherically driven rates of water use in this system and the overall lack of drought stress during the simulation period. Atmospherically driven evapotranspiration rates have been described in other hydrologic studies in grasslands of Argentina [*Varni et al.*, 1999]. The results pre-

sented here therefore suggest that in areas of the Pampas with precipitation excess or in wet zones where evaporation rates scale with available energy, LAI values and morphological characteristics regulating canopy vapor and hydraulic conductance will likely mediate the hydrologic impact of plantations in these grasslands [*Calder*, 1998].

[45] For species requiring direct groundwater withdrawals to meet transpiration demands, hydraulic conductivity of soils in the Pampas may control the aerial extent and productivity of plantations. The soil saturated conductivity controls the distance over which Darcian flow from the surrounding grassland can recharge plantation groundwater levels on daily timescales. Decreasing conductivity values will therefore result in deepening water tables beneath plantations during periods when evapotranspiration is greater than precipitation and groundwater inputs. The model simulations suggest soil hydraulic conductivity may have declined with depth at our study site, since maintaining a constant conductivity in all soil layers led to an overestimate of plantation z 20–40 cm higher than observations during the last part of the simulation period. On the other hand, simulations with significant reductions in hydraulic conductivity from baseline values led to a rapid depletion of plantation water tables beneath the −6 m boundary as transpiration increased during the dry season. Increasing the distance from the input grassland z implicit in the 1-D model environment caused a similar rapid depletion of water tables beneath the plantation. Together, these results agree with those of *Jobbágy and Jackson* [2004] suggesting that water stress in the center of large plantations located in areas of low aquifer transmissivity may limit productivity for phreatophytic tree species. Further studies on water use patterns in *Eucalyptus* plantations in areas of the Pampas characterized by differing soil types, precipitation regimes and groundwater resources should help test this prediction and the hydrological interactions surrounding it.

Appendix A: Model Description

[46] We employed the SPA canopy model [*Williams et al.*, 1996] with updated root functions [*Williams et al.*, 2001] and soil column subroutines [*Stieglitz et al.*, 1997; *Engel et al.*, 2002] to simulate plantation hydrology. SPA is an n-layer canopy model that has been applied in diverse ecosystems and validated with canopy-scale fluxes of latent energy and CO_2. [*Williams et al.*, 1996, 2001] For each canopy layer, an iterative function simultaneously determines photosynthesis and Penman-Monteith transpiration rates for sunlit and shaded leaves. The model employs hydraulic constraints on leaf conductance using a threshold parameter (i) governing stomatal sensitivity to a prescribed minimum midday leaf water potential (Ψ_L, MPa) and water use efficiency. Lower prescribed Ψ_L results in increased drought tolerance and increased ability to withdraw water from a drying soil column. Subroutines for calculating throughfall and interception of precipitation as well as evaporation from wet leaves were retained from *Williams et al.* [1996]. The formulations of root resistances were adopted from *Williams et al.* [2001] and include both axial and radial components. In this scheme, the belowground hydraulic resistance to transpiration uptake in each soil layer is a function of root resistance and volumetric water content. Transpiration demand calculated at the leaf surface is withdrawn from the soil following a distribution based on the fraction of total belowground hydraulic resistance (soil plus roots) in each soil layer. Larger fractions of source water are therefore withdrawn from soil layers with lower hydraulic resistance. A complete description of the belowground subroutines is given by *Williams et al.* [2001].

[47] Soil properties and physical processes are represented with a modified version of the n-layer soil column described by *Stieglitz et al.* [1997]. A five-layer model was employed with a lower boundary condition at −6 m. Individual layer thickness and mineral fractions were estimated from soil core observations at the study site (Tables 3 and 4). Within the soil column, diffusion and a modified tipping bucket model govern heat and water flow, respectively, with modified subroutines controlling upward movement of water due to capillary forces. Within each time step z is updated first based on precipitation infiltration, transpiration withdrawals and local groundwater fluxes. Capillary transport at K_θ moves water from saturated zones upward to soil layers with matric potentials less than the equilibrium values calculated from the elevation above the water table. Then z is lowered by an amount equivalent to that redistributed through capillarity and the updated value is carried into the next model time step. During drainage, the amount of water removed from each soil layer is equivalent to the excess above either field capacity or the equilibrium matric potential, whichever is greater.

[48] Lowering total porosity relative to field capacity controlled SY values in the 5 soil layers. This modification is consistent with the determination of z within individual soil layers in the model environment [*Stieglitz et al.*, 1997]. Groundwater inputs to the plantation from the surrounding grassland are calculated using Darcy's law assuming conditions of a homogeneous unconfined aquifer and are added directly to the soil layer containing the free water surface. At each time step grassland z is used as an input and Darcian flow is calculated as $K_{sat}(dh/L)$, where dh is the difference in elevation head between the input grassland value and the modeled plantation z, L is the distance (200 m) between the two monitoring wells, and K_{sat} was estimated from the well test results. Discharge at the −6 m lower model boundary layer was estimated from groundwater recession rates observed at the grassland monitoring well. The recession rates were calculated during periods of little to no rainfall when z was below the approximate 1.5 m of rooting depth influence of grassland species. A constant discharge of $\sim 2.0 \times 10^{-8}$ m s^{-1} produced the best match with observations.

Notation

E	transpiration, mm d^{-1}.
E_{gw}	transpiration derived from groundwater withdrawals, mm d^{-1}.
K_{sat}	saturated hydraulic conductivity, m s^{-1}.
LAI	leaf area index, m^2 m^{-2}.
θ	soil moisture content, cm^3 cm^{-3}.
U	sap flux density, kg m^{-2} s^{-1}.
z	depth to water table, cm.
$\delta z/\delta t$	change in plantation water table depth from 0000 to 0400 hrs, m d^{-1}.

δz_{ref} net daily changes in the reference monitoring well, m d^{-1}.
δz_{pl} net change in plantation water table depth over a 24 hr period, m d^{-1}.
δz sum of fluxes contributing to groundwater fluctuations, $\delta z/\delta t + \delta z_{ref} + \delta z_{pl}$.
SAI sapwood area index, m^2 m^{-2}.
SY sediment specific yield, m mm^{-1}.

[49] **Acknowledgments.** This research was supported by grants from the InterAmerican Institute for Global Change (SGP 004 and CRN 012), the Fundación Antorchas, NSF, and the Andrew W. Mellon foundation. EGJ has a career fellowship from CONICET, Argentina. Very helpful field assistance was provided by Pedro Gundel, Marcelo Nosetto, Marisa Nordenstahl, Carlos Villardi, and Maria Pilar Clavijo. Special thanks go to Ruben and Alicia Levin for their hospitality and generosity.

References

Amoozegar, A., and A. W. Warrick (1986), Hydraulic conductivity of saturated soils: Field methods, in *Methods of Soil Analysis*, part 1, *Physical and Mineralogical Methods*, edited by A. Klute, pp. 753–770, Soil Sci. Soc. of Am., Madison, Wis.

Bari, M. A., and N. J. Schofield (1992), Lowering of a shallow, saline watertable by extensive eucalypt reforestation, *J. Hydrol.*, *133*, 273–291.

Bauer, P., G. Thaberg, F. Stauffer, and W. Kinzelbach (2004), Estimation of evapotranspiration rate from diurnal groundwater level fluctuations in the Okavango Delta, Botswana, *J. Hydrol.*, *288*, 344–355.

Bramley, H., J. Hutson, and S. D. Tyerman (2003), Floodwater infiltration through root channels on a sodic clay floodplain and the influence on a local tree species *Eucalyptus largiflorens*, *Plant Soil*, *253*, 275–286.

Calder, I. R. (1998), Water use by forests, limits and controls, *Tree Physiol.*, *18*, 625–631.

Calder, I. R., R. L. Hall, and K. T. Prasanna (1993), Hydrologic impact of *Eucalyptus* plantation in India, *J. Hydrol.*, *150*, 249–256.

Clearwater, M. J., F. C. Meinzer, J. L. Andrade, G. Goldstein, and N. M. Holbrook (1999), Potential errors in measurement of nonuniform sap flow using heat dissipation probes, *Tree Physiol.*, *19*(10), 681–687.

Cramer, V. A., and R. J. Hobbs (1992), Ecological consequences of altered hydrologic regimes in fragmented ecosystems in southern Australia: Impacts and possible management responses, *Aust. Ecol.*, *27*, 546–564.

Cramer, V. A., P. J. Thorburn, and G. W. Fraser (1999), Transpiration and groundwater uptake from farm forest plots of *Casuarina glauca* and *Eucalyptus camaldulensis* in saline areas of southeast Queensland, Australia, *Agric. Water Manage.*, *39*, 187–204.

Engel, V. C., M. Stieglitz, M. Williams, and K. L. Griffin (2002), Forest canopy hydraulic properties and catchment water balance: Observations and modeling, *Ecol. Modell.*, *154*, 263–288.

Farley, K. A., E. G. Jobbágy, and R. B. Jackson (2005), Effects of afforestation on water yield: A global synthesis with implications for policy, *Global Change Biol.*, in press.

Farrington, P., G. D. Watson, G. A. Bartle, J. D. Beresford, and E. A. N. Greenwood (1990), Evaporation from dampland vegetation on a groundwater mound, *J. Hydrol.*, *115*, 65–75.

Freeze, R. A., and J. A. Cherry (1986), *Groundwater*, 604 pp., Prentice-Hall, Upper Saddle River, N. J.

Gill, R. A., and R. B. Jackson (2000), Global patterns of root turnover for terrestrial ecosystems, *New Phytol.*, *147*, 13–31.

Granier, A. (1987), Evaluation of transpiration in a Douglas-fir stand by means of sap flow measurements, *Tree Physiol.*, *3*, 309–320.

Granier, A., V. Bobay, J. H. C. Gash, J. Gelpe, B. Sugier, and W. J. Shuttleworth (1990), Vapour flux density and transpiration rate comparisons in a stand of Maritime pine (*Pinus pinaster* Ait) in Les Landes forest, *Agric. For. Meteorol.*, *51*, 309–319.

Gyenge, J. E., M. E. Fernandez, G. Dalla Salda, and T. M. Schlichter (2002), Silvopastoral systems in northwestern Patagonia II: Water balance and water potential in a stand of *Pinus ponderosa* and native grassland, *Agrofor. Syst.*, *55*, 47–55.

Herron, N., R. Davis, and R. Jones (2002), The effects of large-scale afforestation and climate change on water allocation in the Macquarie River catchment, NSW, Australia, *J. Environ. Manage.*, *65*, 369–381.

Heuperman, A. (1999), Hydraulic gradient reversal by trees in shallow water table areas and repercussions for the sustainability of tree growing systems, *Agric. Water Manage.*, *39*, 153–167.

Jackson, R. B., S. R. Carpenter, C. N. Dahm, D. M. McKnight, R. J. Naiman, S. L. Postel, and S. W. Running (2001), Water in a changing world, *Ecol. Appl.*, *11*, 1027–1045.

Jackson, R. B., J. L. Banner, E. G. Jobbágy, W. T. Pockman, and D. H. Wall (2002), Ecosystem carbon loss with woody plant invasion of grasslands, *Nature*, *418*, 623–626.

Jobbágy, E. G. (2002), The imprint of plants on the vertical distribution of soil resources, Ph.D. dissertation, 162 pp., Duke Univ., Durham, N. C.

Jobbágy, E. G., and R. B. Jackson (2003), Patterns and mechanisms of soil acidification in the conversion of grasslands to forests, *Biogeochemistry*, *54*, 205–229.

Jobbágy, E. G., and R. B. Jackson (2004), Groundwater use and salinization with grassland afforestation, *Global Change Biol.*, *10*, 1299–1312.

Jones, H. G. (1992), *Plants and Microclimate: A Quantitative Approach to Environmental Plant Physiology*, 2nd ed., 428 pp., Cambridge Univ. Press, New York.

LeMaitre, D. C., D. F. Scott, and C. Colvin (1999), A review of information on interactions between vegetation and groundwater, *Water Sci. Appl.*, *25*, 137–152.

Mahmood, K., J. Morris, J. Collopy, and P. Slavich (2001), Groundwater uptake and sustainability of farm plantations on saline sites in Punjab province, Pakistan, *Agric. Water Manage.*, *48*, 1–20.

Mather, A. S. (1993), *Afforestation: Policies, Planning, and Progress*, Belhaven, London.

McElrone, A. J., W. T. Pockman, J. Martinez-Vilalta, and R. B. Jackson (2004), Variation in xylem structure and function in stems and roots of trees to 20 m depth, *New Phytol.*, *163*, 507–517.

Mensforth, L. J., P. J. Thorburn, S. D. Tyerman, and G. R. Walker (1994), Sources of water used by riparian *Eucalyptus camaldulensis* overlying highly saline groundwater, *Oecologia*, *100*, 21–28.

Morris, J. D., and J. J. Collopy (1999), Water use and salt accumulation by *Eucalyptus camaldulensis* and *Casuarina cunninghamiana* on a site with shallow saline groundwater, *Agric. Water Manage.*, *39*, 205–227.

Perelman, S. B., R. J. C. Leon, and M. Oesterheld (2001), Cross-scale vegetation patterns of flooding Pampa grasslands, *J. Ecol.*, *89*, 562–577.

Phillips, N., R. Oren, and R. Zimmerman (1996), Radial patterns of xylem sap flow in non-, diffuse-, and ring-porous tree species, *Plant Cell Environ.*, *19*, 983–990.

Richardson, D. M. (1998), Forestry trees as invasive aliens, *Conserv. Biol.*, *12*(1), 18–26.

Salama, R. B., G. A. Bartle, and P. Farrington (1994), Water use of plantation *Eucalyptus camaldulensis* estimated by groundwater hydrograph separation techniques and heat pulse method, *J. Hydrol.*, *156*, 163–180.

Servicio Provincial de Agua Potable y Saneamiento Rural (1987), Perforaciones de explotación en las localidades de Castelli y Lezama, *Rep. 2419-2596/87*, Minist. de Obras Públicas, Prov. de Buenos Aires, Buenos Aires.

Soriano, A. (1991), Rio de la Plata grasslands, in *Natural Grasslands: Ecosystems of the World*, pp. 367–405, Elsevier, New York.

Stieglitz, M., D. Rind, J. Famiglietti, and C. Rosenzweig (1997), An efficient approach to modeling the topographic control of surface hydrology for regional and global climate modeling, *J. Clim.*, *10*, 118–137.

Thorburn, P. J., and G. R. Walker (1994), Variations in stream water uptake by *Eucalyptus camaldulensis* with differing access to stream water, *Oecologia*, *100*, 293–301.

Thorburn, P. J., T. J. Hatton, and G. R. Walker (1993), Combining measurements of transpiration and stable isotopes of water to determine groundwater discharge from forests, *J. Hydrol.*, *150*, 563–587.

Tricart, J. L. (1973), *Geomorfologia de la Pampa Deprimida: Base Para lose Studios Edafologicos y Agronomicos*, *Colession Cient.*, vol. 12, 202 pp., Inst. Nac. de Tecnol. Agropecuaria, Buenos Aires.

Varni, M., E. Usunoff, P. Weinzettal, and R. Rivas (1999), Groundwater recharge in the Azul aquifer, Central Buenos Aires Province, Argentina, *Phys. Chem. Earth B*, *24*(4), 349–352.

Vertessy, R., L. Connell, J. Morris, R. Silberstein, A. Heuperman, P. Feikema, L. Mann, M. Komarzynski, J. Collopy, and D. Stackpole (2000), Sustainable hardwood production in shallow water table areas, *Publ. 00-163*, Rural Ind. Res. and Dev. Corp., Barton, A. C. T., Australia.

White, W. N. (1932), A method of estimating groundwater supplies based on discharge by plants and evaporation from soil, *U.S. Geol. Surv. Water Supply Pap.*, *659-A*.

Williams, M. (1990), Forests, in *The Earth as Transformed by Human Action*, edited by B. L. Turner II et al., pp. 179–201, Cambridge Univ. Press, New York.

Williams, M., E. B. Rastetter, D. N. Fernandes, M. L. Goulden, S. C. Wofsy, G. R. Shaver, J. M. Melillo, J. W. Munger, S. M. Fan, and K. J. Nadelhoffer (1996), Modelling the soil-plant-atmosphere continuum in a *Quercus-Acer* stand at Harvard Forest: The regulation of stomatal conductance by light, nitrogen, and soil/plant hydraulic properties, *Plant Cell Environ.*, *21*, 953–968.

Williams, M., B. E. Law, P. M. Anthoni, and M. H. Unsworth (2001), Use of a simulation model and ecosystem flux data to examine carbon-water interactions in ponderosa pine, *Tree Physiol.*, *21*, 287–298.

Wright, J. A., A. DiNicola, and E. Gaitan (2000), Latin American forest plantations—Opportunities for carbon sequestration, economic development, and financial returns, *J. For.*, *98*, 20–23.

Zárate, M. A. (2003), Loess of southern South America, *Quat. Sci. Rev.*, *22*, 1987–2006.

V. Engel, National Park Service, Everglades National Park, 950 North Krome Avenue, Homestead, FL 33030, USA. (vic_engel@nps.gov)

R. B. Jackson, Department of Biology, Duke University, Durham, NC 27708, USA.

E. G. Jobbágy, GEA, IMASL, Universidad Nacional de San Luis, Ej de los Andes 950, 5700 San Luis, Argentina.

M. Stieglitz, Department of Civil and Environmental Engineering, Georgia Institute of Technology, 790 Atlantic Drive, Atlanta, GA 30332-0355, USA.

M. Williams, Institute of Atmospheric and Environmental Sciences, University of Edinburgh, Crew Building, Edinburgh EH9 3JN, UK.